

CrossMark  
click for updatesCite this: *Chem. Sci.*, 2016, 7, 1142

# Negative ion photoelectron spectroscopy confirms the prediction that $D_{3h}$ carbon trioxide ( $\text{CO}_3$ ) has a singlet ground state†

David A. Hrovat,<sup>a</sup> Gao-Lei Hou,<sup>b</sup> Bo Chen,<sup>a</sup> Xue-Bin Wang<sup>\*b</sup>  
and Weston Thatcher Borden<sup>\*a</sup>

The  $\text{CO}_3$  radical anion ( $\text{CO}_3^{\cdot-}$ ) has been formed by electro spraying carbonate dianion ( $\text{CO}_3^{2-}$ ) into the gas phase. The negative ion photoelectron (NIPE) spectrum of  $\text{CO}_3^{\cdot-}$  shows that, unlike the isoelectronic trimethylenemethane [ $\text{C}(\text{CH}_2)_3$ ],  $D_{3h}$  carbon trioxide ( $\text{CO}_3$ ) has a singlet ground state. From the NIPE spectrum, the electron affinity of  $D_{3h}$  singlet  $\text{CO}_3$  was, for the first time, directly determined to be  $\text{EA} = 4.06 \pm 0.03$  eV, and the energy difference between the  $D_{3h}$  singlet and the lowest triplet was measured as  $\Delta E_{\text{ST}} = -17.8 \pm 0.9$  kcal mol<sup>-1</sup>. B3LYP, CCSD(T), and CASPT2 calculations all find that the two lowest triplet states of  $\text{CO}_3$  are very close in energy, a prediction that is confirmed by the relative intensities of the bands in the NIPE spectrum of  $\text{CO}_3^{\cdot-}$ . The 560 cm<sup>-1</sup> vibrational progression, seen in the low energy region of the triplet band, enables the identification of the lowest, Jahn–Teller-distorted, triplet state as  $^3A_1$ , in which both unpaired electrons reside in  $\sigma$  MOs, rather than  $^3A_2$ , in which one unpaired electron occupies the  $b_2$   $\sigma$  MO, and the other occupies the  $b_1$   $\pi$  MO.

Received 19th September 2015

Accepted 2nd November 2015

DOI: 10.1039/c5sc03542b

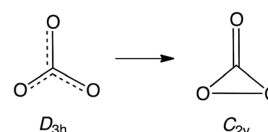
www.rsc.org/chemicalscience

## Introduction

Carbon trioxide,  $\text{CO}_3$ , is an unusual molecule with a long history. In 1962  $\text{CO}_3$  was proposed by Katakis and Taube to be an intermediate in photoreaction of  $\text{O}_3$  with  $\text{CO}_2$ .<sup>1</sup> Four years later,  $\text{CO}_3$  was again postulated as a reactive intermediate, this time in the photoreaction of  $\text{CO}_2$  with itself.<sup>2</sup>

Experimental confirmation of the existence of  $\text{CO}_3$  was obtained by IR spectroscopy on the matrix-isolated molecule, first by Moll, Clutter and Thompson in 1966,<sup>3</sup> and subsequently by Weissberger, Breckenridge and Taube in 1967 (ref. 4) and by Jacox and Milligan in 1971.<sup>5</sup> These experiments favored a  $C_{2v}$  structure for  $\text{CO}_3$ , containing a three-membered O–C–O ring and a carbonyl group. Nevertheless, a higher energy,  $D_{3h}$  isomer

was detected by Kaiser and coworkers in 2006.<sup>6</sup> Very recently, the  $C_{2v}$  and  $D_{3h}$  isomers were reported by Sivaraman and coworkers to coexist in ion-irradiated  $\text{CO}_2$  ice.<sup>7</sup>



A number of theoretical studies from the 1960s to 1980s investigated the structure of  $\text{CO}_3$ , mainly focusing on relative stabilities of the cyclic  $C_{2v}$  structure, the acyclic  $C_s$  structure, and the linear  $C_{\infty v}$  structure.<sup>8</sup> These INDO, EH, SCF, and MP2 calculations all found that the  $C_{2v}$  isomer is the lowest in energy.<sup>9</sup>

Nevertheless, in 1987 CISD calculations by Mulder and coworkers found the  $D_{3h}$  structure to be lower in energy than the  $C_{2v}$  structure.<sup>10</sup> However, subsequent calculations at higher levels of theory agree that the ground state of  $\text{CO}_3$  possesses a  $C_{2v}$  structure, which is computed to be 1.8–6.4 kcal mol<sup>-1</sup> lower in energy than the  $D_{3h}$  isomer.<sup>11</sup> A small barrier of 4.0–8.6 kcal mol<sup>-1</sup> is calculated for the isomerization from the  $C_{2v}$  to  $D_{3h}$  structure.<sup>11b,e,12</sup> The computational finding of separate  $C_{2v}$  and  $D_{3h}$  minima, with the former lower in energy than the latter, is, of course, consistent with the results of the experiments on matrix-isolated  $\text{CO}_3$ .<sup>3–7</sup>

The singlet-triplet energy difference ( $\Delta E_{\text{ST}}$ ) in  $\text{CO}_3$  has also been computed.  $\Delta E_{\text{ST}}$  between the  $^1A_1$  singlet ground state and the  $^3A_1$  triplet state at their  $C_{2v}$  equilibrium geometries was

<sup>a</sup>Department of Chemistry and the Center for Advanced Scientific Computing and Modeling, University of North Texas, 1155 Union Circle, #305070, Denton, Texas 76203-5017, USA. E-mail: borden@unt.edu

<sup>b</sup>Physical Sciences Division, Pacific Northwest National Laboratory, P. O. Box 999, MS K8-88, Richland, WA 99352, USA. E-mail: xuebin.wang@pnl.gov

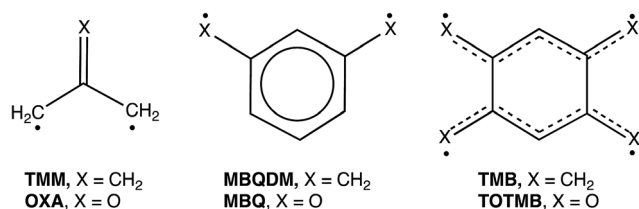
† Electronic supplementary information (ESI) available: Optimized geometries, electronic energies, zero-point vibrational energies, and imaginary frequencies for all of the  $\text{CO}_3$  electronic states discussed in this manuscript, computed with the aug-cc-pVTZ basis set, using B3LYP, CCSD(T), and (16/13)CASPT2 calculations. Fig. S1 contains the CCSD(T) simulation of the triplet region of the NIPE spectrum of  $(\text{CO}_3)^{\cdot-}$  and the assignment of the vibrational progressions in it; Fig. S2 shows the calculated NIPE spectrum, with the lines in the stick spectrum in Fig. S1, convoluted with Gaussians; and Fig. S3 shows how the appearance of the simulation in Fig. 3 is modified by choosing a different value of the energy difference between the 0–0 bands in the two lowest energy triplet states (9 pages). See DOI: 10.1039/c5sc03542b



calculated by fourth-order MBPT calculations to be  $-20.5 \text{ kcal mol}^{-1}$ .<sup>11a</sup> (The negative sign indicates that the singlet is lower in energy than the triplet). Similar values were obtained by QCISD(T) calculations.<sup>11b,g</sup> The  $\Delta E_{\text{ST}}$  of  $\text{CO}_3$  between the  $^1\text{A}_1$  singlet state and a different triplet state ( $^3\text{B}_2$ ) was computed to be  $-22.5 \text{ kcal mol}^{-1}$  at the MRCI+Q(16,13)/6-311+G(3df)//CASSCF(16,13)/6-311G(d) level of theory.<sup>12</sup>

Also of interest have been the roles of  $\text{CO}_3$  in the quenching of the singlet excited state of oxygen atom ( $^1\text{D}$ ) by  $\text{CO}_2$  and in the  $^{18}\text{O}$  enrichment in  $\text{CO}_2$  in the atmospheres of Earth and Mars.<sup>13</sup> Singlet and triplet potential energy surfaces for the reaction of O with  $\text{CO}_2$  have both been calculated.<sup>9,11b,14</sup>

Our own interest in  $\text{CO}_3$  comes from the fact that it is the  $n = 3$  member of the isoelectronic series of  $\text{C}(\text{CH}_2)_{3-n}\text{O}_n$  diradicals, for which  $n = 0$  is trimethylenemethane (**TMM**) and  $n = 1$  is oxyallyl (**OXA**). Negative ion photoelectron spectroscopy (NIPES) has shown that the substitution of the oxygen in **OXA** for one  $\text{CH}_2$  group in **TMM** changes  $\Delta E_{\text{ST}}$  by  $17.5 \text{ kcal mol}^{-1}$ , from  $\Delta E_{\text{ST}} = 16.2 \text{ kcal mol}^{-1}$  for the triplet ground state of **TMM**<sup>15</sup> to  $\Delta E_{\text{ST}} = -1.3 \text{ kcal mol}^{-1}$  for the singlet ground state of **OXA**.<sup>16</sup>



However, the substitution of oxygen for  $\text{CH}_2$  does not always have such a large effect on  $\Delta E_{\text{ST}}$  in diradicals. For example, NIPES has shown that substitution of the oxygens in *meta*-benzoquinone (**MBQ**) for both  $\text{CH}_2$  groups in *meta*-benzoquinodimethane (**MBQDM**) changes  $\Delta E_{\text{ST}}$  by only  $0.6 \text{ kcal mol}^{-1}$ , from  $\Delta E_{\text{ST}} = 9.6 \text{ kcal mol}^{-1}$  in **MBQDM**<sup>17</sup> to  $\Delta E_{\text{ST}} = 9.0 \text{ kcal mol}^{-1}$  in **MBQ**.<sup>18</sup> Substituting the oxygens in 1,2,4,5-tetraoxatetramethylenebenzene (**TOTMB**) for the four methylene groups in tetramethylenebenzene (**TMB**) has been predicted actually to destabilize the singlet, relative to the triplet, decreasing  $\Delta E_{\text{ST}}$  by  $2.7 \text{ kcal mol}^{-1}$ , from a calculated value of  $\Delta E_{\text{ST}} = -6.2 \text{ kcal mol}^{-1}$  in **TMB** to a value of  $\Delta E_{\text{ST}} = -3.5 \text{ kcal mol}^{-1}$ , both calculated for and subsequently found by NIPES in **TOTMB**.<sup>19</sup>

As mentioned above, calculations have predicted a singlet ground state with  $C_{2v}$  geometry for  $\text{CO}_3$ , with  $\Delta E_{\text{ST}}$  values ranging from  $-18.3 \text{ kcal mol}^{-1}$  (ref. 11b) to  $-22.5 \text{ kcal mol}^{-1}$ .<sup>12</sup> However, an experimental measurement of  $\Delta E_{\text{ST}}$  in  $\text{CO}_3$  has not been published.

Similarly, the electron affinity (EA) of  $\text{CO}_3$  has been computed, with the best values ranging from  $\text{EA} = 3.84 \text{ eV}$  to  $\text{EA} = 4.08 \text{ eV}$ .<sup>20</sup> However, the EA of  $\text{CO}_3$  has not been directly measured. With one exception,<sup>21</sup> the experimental estimates are in the range  $\text{EA} = 1.8\text{--}3.5 \text{ eV}$ ,<sup>22</sup> far below the best calculated values.<sup>20</sup>

In order to obtain accurate experimental values for both EA and  $\Delta E_{\text{ST}}$  in  $\text{CO}_3$ , we sought to obtain the NIPES spectrum of  $\text{CO}_3^{\cdot-}$ . Herein we report this spectrum and assign the peaks in it with the help of DFT and *ab initio* calculations. The NIPES spectrum and our analysis of it lead to values of  $\text{EA} = 4.06 \pm$

$0.03 \text{ eV}$ , and  $\Delta E_{\text{ST}} = -17.8 \pm 0.9 \text{ kcal mol}^{-1}$  between the  $D_{3h}$   $^1\text{A}_1'$  state and the Jahn-Teller distorted  $^3\text{E}'$  state.

## Experimental methodology

The NIPES experiments were performed with an apparatus that consisted of an electrospray ionization source, a cryogenic ion trap, and a magnetic-bottle time-of-flight (TOF) photoelectron spectrometer.<sup>23</sup> Electrospraying an aqueous methanolic solution of  $\text{Na}_2\text{CO}_3$  into a vacuum afforded generation of a weak  $\text{CO}_3^{\cdot-}$  radical anion beam, although  $\text{HCO}_3^-$  was always the dominant anion formed.<sup>24</sup> The anions generated were guided by quadrupole ion guides into an ion trap, where they were accumulated and cooled by collisions with cold buffer gas, before being transferred into the extraction zone of a TOF mass spectrometer.

The  $\text{CO}_3^{\cdot-}$  radical anions were carefully mass selected, and decelerated before being photodetached with a laser beam of  $193 \text{ nm}$  ( $6.424 \text{ eV}$ ) from an ArF laser in the photodetachment zone. The laser was operated at a  $20 \text{ Hz}$  repetition rate with the ion beam off at alternating laser shots, to enable shot-to-shot background subtraction to be carried out. Photoelectrons were collected at  $\sim 100\%$  efficiency with the magnetic bottle and analyzed in a  $5.2 \text{ m}$  long electron flight tube.

The TOF photoelectron spectra were converted into electron kinetic energy spectra by calibration with the known NIPE spectra of  $\text{I}^-$  and  $\text{Cu}(\text{CN})_2^-$ . The electron binding energies, given in the spectrum in Fig. 1 were obtained by subtracting the electron kinetic energies from the detachment photon energy.

The best instrumental resolution was  $20 \text{ meV}$  full width at half maximum for  $1 \text{ eV}$  kinetic energy electrons, as demonstrated in the  $\text{I}^-$  spectrum after a maximum deceleration. However, due to the weak mass intensity and light mass of  $\text{CO}_3^{\cdot-}$ , the NIPE spectra of  $\text{CO}_3^{\cdot-}$  were obtained under compromised conditions with  $4\%$  energy resolution, *i.e.*,  $40 \text{ meV}$  for  $1 \text{ eV}$  kinetic energy electrons.

## Computational methodology

In order to help analyze the NIPES spectrum of  $\text{CO}_3^{\cdot-}$ , three different types of electronic structure calculations were

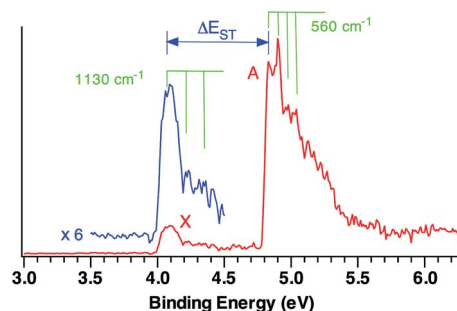


Fig. 1 The  $20 \text{ K}$  NIPES spectrum of  $\text{CO}_3^{\cdot-}$  at  $193 \text{ nm}$  ( $6.424 \text{ eV}$ ). The intensity of the low binding energy band X is *ca.* one sixth of the high binding energy band A. The inset in blue is the X band enlarged by a factor of 6. The spectrum yields values of  $\text{EA} = 4.06 \pm 0.03 \text{ eV}$ , and  $\Delta E_{\text{ST}} = -0.77 \pm 0.04 \text{ eV} = -17.8 \pm 0.9 \text{ kcal mol}^{-1}$ .



performed – B3LYP DFT calculations,<sup>25</sup> CCSD(T) coupled cluster calculations,<sup>26</sup> and (16/13)CASPT2 calculations.<sup>27</sup> In the CASPT2 calculations second-order perturbation theory was used to add the effects of dynamic electron correlation<sup>28</sup> to a (16/13)CASSCF wavefunction. The (16/13)CASSCF active space consisted of all the configurations that can be generated by distributing four valence electrons from carbon and four from each of the three oxygens among 13 MOs. The MOs were those formed from the  $\sigma$  and  $\pi$  2p lone-pair AOs on each oxygen in  $\text{CO}_3$ , the three C–O bonding and three C–O antibonding  $\sigma$  orbitals, and the 2p- $\pi$  AO on carbon.

All of the calculations were performed using the aug-cc-pVTZ basis set.<sup>29</sup> The B3LYP and CCSD(T) calculations and vibrational analyses at these two levels of theory were carried out using the Gaussian09 suite of programs.<sup>30</sup> The CASSCF and CASPT2 calculations were performed with MOLCAS.<sup>31</sup> The program ezSpectrum<sup>32</sup> was used to compute the Franck–Condon factors<sup>33</sup> that were necessary in order to simulate the vibrational progressions in the NIPE spectrum of  $\text{CO}_3^{*-}$ .

## Results and discussion

### The NIPE spectrum of $\text{CO}_3^{*-}$

Fig. 1 shows the 20 K NIPE spectrum of  $\text{CO}_3^{*-}$  at 193 nm. A weak band, X, peaked at electron binding energy (EBE) of  $\sim 4.1$  eV, and a strong band A, peaked at EBE of  $\sim 4.9$  eV, are observed in the spectrum. The intensity of the X band is *ca.* one sixth of the A band.

For statistical reasons, formation of a triplet state is a factor of three more probable than formation of a singlet state; so triplet states invariably give the most intense peaks in NIPE spectra.<sup>34</sup> Thus, the NIPE spectrum of  $\text{CO}_3^{*-}$  indicates that the ground state of  $\text{CO}_3$  is a singlet and that the lowest excited state is a triplet. However, the factor of about six difference between the intensities of the X and A bands in the NIPE spectrum in Fig. 1 suggests that  $\text{CO}_3$  has two triplet states with very similar energies and that both can be formed in the photodetachment of an electron from  $\text{CO}_3^{*-}$ .

From the rising edge of the X band, we estimate the adiabatic detachment energy (ADE) of  $\text{CO}_3^{*-}$  (or, equivalently, the electron affinity, EA of  $\text{CO}_3$ ) to be  $4.06 \pm 0.03$  eV. The EA of  $\text{CO}_3$  has been the subject of many previous experimental studies;<sup>22</sup> but our NIPES value is considerably larger than all but one of these experimental estimates.<sup>21</sup> However, our value of EA =  $4.06 \pm 0.03$  eV is within experimental error of the value of EA = 4.08 eV, calculated at the CCSD(T)/aug-cc-pVTZ level by Cappa and Elrod in 2001.<sup>20</sup>

The experimental singlet–triplet gap of  $\text{CO}_3$ ,  $\Delta E_{\text{ST}}$ , is defined as the difference between the EBE of the X band (EBE =  $4.06 \pm 0.03$  eV) and the EBE of the first resolved peak in the A band (EBE =  $4.83 \pm 0.03$  eV). Therefore,  $\Delta E_{\text{ST}} = -0.77 \pm 0.04$  eV =  $-17.8 \pm 0.9$  kcal mol<sup>-1</sup> is obtained from the NIPE spectrum in Fig. 1.

Vibrational structure can be discerned in both the X and A bands. The ground state X band shows a vibrational progression with a frequency of 1130 cm<sup>-1</sup>. This frequency is high enough

that it is likely to belong to a C–O stretching, rather than to an O–C–O bending mode.

The vibrational mode that appears to be excited in the A band transition has a frequency of 560 cm<sup>-1</sup>. Its low frequency makes it much more likely to be due to an O–C–O bending mode than to a C–O stretching mode.

### The electronic structure of $\text{CO}_3$ – qualitative considerations

Understanding the NIPE spectrum of  $\text{CO}_3^{*-}$  requires understanding the electronic structure of  $\text{CO}_3$ . As already noted,  $D_{3h}$  TMM and  $D_{3h}$   $\text{CO}_3$  are isoelectronic. Therefore, like  $D_{3h}$  TMM,  $D_{3h}$   $\text{CO}_3$  might have been expected to have a triplet ground state. However, as discussed in the previous section, the NIPE spectrum of  $\text{CO}_3^{*-}$  shows that the ground state of  $D_{3h}$   $\text{CO}_3$  is a singlet and that  $\Delta E_{\text{ST}} = -17.8 \pm 0.9$  kcal mol<sup>-1</sup>.

The reason that TMM has a triplet ground state is that in  $D_{3h}$  TMM two electrons occupy two degenerate,  $e''$ ,  $\pi$  MOs. The MOs are non-disjoint;<sup>35</sup> therefore, as expected from Hund's rule,<sup>36</sup> the triplet is the electronic state of lowest energy.<sup>16</sup>

However, the C–H bonds in  $D_{3h}$  TMM are replaced by  $\sigma$  lone pairs of electrons on the three oxygens of  $\text{CO}_3$ . As shown in Fig. 2, the  $a_2'$  combination of oxygen lone pair orbitals is antibonding between all three oxygens. Therefore, in the lowest electronic state of  $D_{3h}$   $\text{CO}_3$ , the  $a_2'$  MO is left empty.

The pair of electrons that occupy the  $a_2'$  C–H bonding MO in  $D_{3h}$  TMM reside in one of the pair of  $e''$   $\pi$  MOs in  $D_{3h}$   $\text{CO}_3$ . Consequently, a total of four electrons occupy the  $e''$ ,  $\pi$  MOs in  $D_{3h}$   $\text{CO}_3$ , and four more electrons occupy the degenerate pair of  $e'$ ,  $\sigma$  MOs. This is the reason why the lowest electronic state of  $D_{3h}$   $\text{CO}_3$  is a closed-shell singlet.

In the  $\text{CO}_3^{*-}$  radical anion one electron occupies the  $a_2'$  MO. In the low energy triplet states of neutral  $\text{CO}_3$  one electron in the closed-shell, singlet, ground state is excited into this MO.

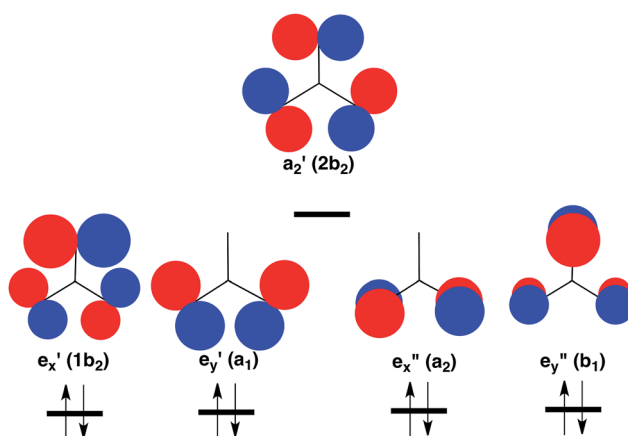


Fig. 2 Schematic depiction of the three  $\sigma$  and two  $\pi$  lone-pair MOs of highest energy that are localized on the three oxygens in  $\text{CO}_3$ . Symmetries of these MOs are given at  $D_{3h}$  and ( $C_{2v}$ ) geometries. Of these MOs,  $a_2'$  is highest in energy, because it contains antibonding  $\sigma$  interactions between all three oxygens. Therefore,  $a_2'$  is left empty and the degenerate pairs of  $e'$  and  $e''$  MOs are each doubly occupied in the closed-shell singlet ground state of  $\text{CO}_3$ .<sup>37</sup> The orbital occupancy in this  $^1A_1$  state is indicated at the bottom of Fig. 2.



**Table 1** Calculated B3LYP,<sup>25</sup> CCSD(T),<sup>26</sup> and CASPT2 (ref. 27) energies (kcal mol<sup>-1</sup>) of the ground state of CO<sub>3</sub><sup>-</sup> and of the low-lying electronic states of CO<sub>3</sub>, relative to the D<sub>3h</sub> <sup>1</sup>A<sub>1</sub> state of CO<sub>3</sub>. Calculations were carried out with the aug-cc-pVTZ basis set.<sup>29</sup> Electronic states and orbital occupancies after Jahn–Teller distortions to C<sub>2v</sub> symmetry of the two components of <sup>3</sup>E' and <sup>3</sup>E'' states are given in parentheses, and the energies after the Jahn–Teller distortions are indicated by arrows

Electronic state	B3LYP	CCSD(T)	CASPT2
<sup>2</sup> A <sub>2</sub> ' of CO <sub>3</sub> <sup>-</sup>	-116.4 (-5.05 eV)	-95.4 (-4.13 eV) <sup>a</sup>	-93.9 (-4.07 eV)
<sup>1</sup> A <sub>1</sub> ' (D <sub>3h</sub> minimum)	0	0 <sup>b</sup>	0
<sup>1</sup> A <sub>1</sub> (C <sub>2v</sub> TS) <sup>c</sup>	0.6	1.5	6.6
<sup>1</sup> A <sub>1</sub> (C <sub>2v</sub> minimum containing an O–C–O ring)	-13.4	-5.5	-2.2
<sup>3</sup> E <sub>x</sub> ' ( <sup>3</sup> B <sub>2</sub> =  ...a <sub>1</sub> <sup>2</sup> b <sub>2</sub> <sup>2</sup> >)	-1.0 → -4.2	19.1 → 16.3	24.8 → 21.0
<sup>3</sup> E <sub>y</sub> ' ( <sup>3</sup> A <sub>1</sub> =  ...1b <sub>2</sub> <sup>2</sup> 2b <sub>2</sub> <sup>2</sup> >)	-1.0 → -3.6	18.6 → 15.5	23.7 → 20.8
<sup>3</sup> E <sub>x</sub> ' ( <sup>3</sup> A <sub>2</sub> =  ...b <sub>1</sub> <sup>2</sup> 2b <sub>2</sub> <sup>2</sup> >)	1.0 → -1.0	19.5 → 17.8	20.1 → 19.8
<sup>3</sup> E <sub>y</sub> ' ( <sup>3</sup> B <sub>1</sub> =  ...a <sub>2</sub> <sup>2</sup> 2b <sub>2</sub> <sup>2</sup> >)	-0.6 → -0.7	19.5 → 19.2	20.2 → 19.3
<sup>3</sup> A <sub>2</sub> ' ( <sup>3</sup> B <sub>2</sub> =  ...b <sub>1</sub> <sup>2</sup> a <sub>2</sub> <sup>2</sup> >)	11.7	28.4	35.9

<sup>a</sup> Previous calculations at this level of theory obtained -4.08 eV for the EA of CO<sub>3</sub>.<sup>20</sup> <sup>b</sup> Artificial symmetry breaking<sup>39–41</sup> results in this state having two imaginary frequencies for distortions that lead to three equivalent C<sub>2v</sub> minima. These minima have CCSD(T) energies that are 0.9 kcal mol<sup>-1</sup> lower than that of the D<sub>3h</sub> singlet state. <sup>c</sup> One of three transition structures that connect the D<sub>3h</sub> singlet to one of the three C<sub>2v</sub> structures that are the global minima on the potential energy surface for the lowest singlet state of CO<sub>3</sub>.

However, whether the electron that occupies the a<sub>2</sub>' MO in the triplet comes from one of the e' σ MOs or one of the e'' π MOs in the singlet is not obvious. The question of the relative energies of the resulting <sup>3</sup>E' and <sup>3</sup>E'' states of CO<sub>3</sub> has been addressed by the calculations that are described in a later section of this paper.

### Computational results for the lowest singlet state of CO<sub>3</sub>

The results of our B3LYP, CCSD(T), and CASPT2 calculations on CO<sub>3</sub><sup>-</sup> and CO<sub>3</sub> are summarized in Table 1. All of these calculations find that in the lowest electronic state of the radical anion the unpaired electron occupies the a<sub>2</sub> MO, so that CO<sub>3</sub><sup>-</sup> maintains D<sub>3h</sub> symmetry.<sup>38</sup> The B3LYP and CASPT2 calculations find that the D<sub>3h</sub> singlet state is also an energy minimum.

However, the CCSD(T) calculations find that the D<sub>3h</sub> geometry of the <sup>1</sup>A<sub>1</sub>' state has two imaginary frequencies of 472i cm<sup>-1</sup>. These correspond to a degenerate pair of e' vibrations that lead to a trio of slightly distorted structures with C<sub>2v</sub> symmetry (not to be confused with the cyclic C<sub>2v</sub> structure with an O–C–O ring and a carbonyl group). The three equivalent C<sub>2v</sub> structures are 0.9 kcal mol<sup>-1</sup> lower in energy than the D<sub>3h</sub> structure at the CCSD(T)/aug-cc-pVTZ level of theory.

When the basis set is expanded to aug-cc-pVQZ, the energy difference between the D<sub>3h</sub> and C<sub>2v</sub> structures drops to only 0.3 kcal mol<sup>-1</sup>. Since the B3LYP and the CASPT2 calculations both find the D<sub>3h</sub> structure to be an energy minimum, we believe that the small geometry distortions to structures with C<sub>2v</sub> symmetry in the CCSD(T) calculations are due to artificial symmetry breaking in the CCSD(T) wave function for the <sup>1</sup>A<sub>1</sub>' state at D<sub>3h</sub> geometries.<sup>39–41</sup>

If the lowest electronic states of CO<sub>3</sub><sup>-</sup> and CO<sub>3</sub> both have D<sub>3h</sub> symmetry, it is possible to assign the vibrational progression in the X band of the NIPE spectrum in Fig. 1 to a symmetrical C–O stretching mode. Only vibrational modes that preserve those symmetry elements that the electronic states of the radical ion and the neutral molecule have in common are

seen in NIPE spectra. Therefore, the vibrational progression with a frequency of 1130 cm<sup>-1</sup> that is seen in the X band in Fig. 1 must belong to the a<sub>1</sub>' vibration of D<sub>3h</sub> CO<sub>3</sub>.

On going from the CO<sub>3</sub><sup>-</sup> radical anion to neutral CO<sub>3</sub> the C–O bond lengths are calculated to shorten by 0.013 Å (CASPT2), 0.015 Å [CCSD(T)], and 0.023 Å (UB3LYP). Consequently, the calculated Franck–Condon factors predict that an a<sub>1</sub>' C–O bond stretching vibrational progression should be seen in the X band in Fig. 1. The calculated harmonic frequencies for the a<sub>1</sub>' C–O stretching vibration are 1083 cm<sup>-1</sup> (CASPT2), 1090 cm<sup>-1</sup> [CCSD(T)] and 1140 cm<sup>-1</sup> (B3LYP). The B3LYP value differs by only 10 cm<sup>-1</sup> from the experimental value of 1130 cm<sup>-1</sup>.

Since the 1130 cm<sup>-1</sup>, a<sub>1</sub>', C–O bond stretching mode is totally symmetric, it would not have been seen in the IR spectrum of D<sub>3h</sub> CO<sub>3</sub> in matrix isolation. The observed, asymmetric (e'), C–O bond-stretching frequency was reported to be 1165 cm<sup>-1</sup>.<sup>6</sup>

As shown in Table 1, and, in agreement with the results of previous calculations<sup>11</sup> and experiments,<sup>3–7</sup> B3LYP, CCSD(T), and CASPT2 all find that there is a C<sub>2v</sub> singlet energy minimum, containing an O–C–O ring, that is lower in energy than the D<sub>3h</sub> singlet. Not unexpectedly, the barrier height that is calculated for ring closure increases as the calculated exothermicity of this reaction decreases.

Because the D<sub>3h</sub> → C<sub>2v</sub> ring closure reaction requires mixing of the filled e' MOs in Fig. 2 with the empty a<sub>2</sub>' MO, ring closure is computed to involve passage over a barrier. This orbital mixing, which occurs on an e' distortion from D<sub>3h</sub> to C<sub>2v</sub> symmetry, may be regarded as a second-order Jahn–Teller effect.<sup>42</sup>

For example, at C<sub>2v</sub> geometries e<sub>x</sub>' and a<sub>2</sub>' both have b<sub>2</sub> symmetry and so can be mixed by an e<sub>y</sub> distortion from D<sub>3h</sub> symmetry. From inspection of the MOs in Fig. 2, one can deduce that this mixing reduces the contribution of the AOs on the two oxygens between which O–O bond formation occurs and thus makes the resulting b<sub>2</sub> MO much less antibonding than the e<sub>x</sub>' MO. In fact, the b<sub>2</sub> MO that results from the mixing between



$e'_x$  and  $a'_2$  MOs becomes the  $2p_x$  lone-pair AO on the carbonyl group of the  $C_{2v}$  singlet energy minimum.

The large change in geometry that occurs on formation of the cyclic singlet  $CO_3$  molecule results in the absence of overlap between its vibrational wave function and the vibrational wave function of the  $D_{3h}$   $CO_3^{\cdot-}$  radical anion. Consequently, the Franck–Condon factor for the laser-induced transition from  $D_{3h}$   $CO_3^{\cdot-}$  to the  $C_{2v}$  energy minimum of singlet  $CO_3$  is calculated to be effectively zero. Therefore, the value of  $EA = 4.06 \pm 0.03$  eV in the NIPE spectrum corresponds to the energy difference between the  $D_{3h}$  equilibrium geometry of  $CO_3^{\cdot-}$  and the local  $D_{3h}$  energy minimum of neutral singlet  $CO_3$ , not the global  $C_{2v}$  energy minimum, of singlet,  $CO_3$ .

There are two types of experimental evidence that support this conclusion. The first is that the measured EA is very close to the calculated CCSD(T) and CASPT2 energy differences in Table 1 between the  $D_{3h}$  equilibrium geometry of  $CO_3^{\cdot-}$  and the local  $D_{3h}$  energy minimum of neutral  $CO_3$ . Second, as already discussed, the vibrational progression of  $1130\text{ cm}^{-1}$  seen in the X band of the NIPE spectrum in Fig. 1 is in good agreement with that predicted by all three levels of theory for the  $D_{3h}$  local minimum.

### Computational results for the lowest triplet state of $CO_3$

As shown in Table 1, there are two low-lying triplet states in  $CO_3$ . They are  $E'$ , in which the two unpaired electrons occupy the  $a'_2$  and  $e'$   $\sigma$  MOs, and  $E''$ , in which the second unpaired electron occupies the  $e''$   $\pi$  MO, instead of the  $e'$   $\sigma$  MO.

A third triplet,  ${}^3A'_2$ , which is the ground state of TMM, is calculated to be very high in energy in  $CO_3$ . In this state the  $e'_x$  and  $e'_y$   $\pi$  MOs are each singly occupied, and the  $a'_2$  MO is doubly occupied. As shown in Fig. 2, the  $a'_2$  MO is strongly O–O antibonding; and its double occupancy in  ${}^3A'_2$  makes this triplet state much higher in energy than either  ${}^3E'$  or  ${}^3E''$ , in both of which the  $a'_2$  MO is singly occupied.

Whether  ${}^3E'$  or  ${}^3E''$  is lower in energy is not clear from qualitative considerations. As shown in Fig. 2, the  $e'$  MOs are weakly bonding  $\sigma$  MOs; whereas, the  $e''$  MOs are non-bonding  $\pi$  MOs. On this basis, leaving  $e'$  doubly occupied and having  $e''$  singly occupied should be favored; so  ${}^3E''$  should be lower in energy than  ${}^3E'$ .

On the other hand, two electrons of the same spin cannot simultaneously occupy the same AO. With one electron in the  $a'_2$   $\sigma$  MO, having a second electron of the same spin in an  $e'$   $\sigma$  MO prevents these two electrons from ever appearing on the same atom; whereas, no such prohibition exists if the second unpaired electron occupies an  $e''$   $\pi$  MO. Consequently, although maximization of bonding is expected to favor the  ${}^3E''$  state, minimization of electron repulsion should favor the  ${}^3E'$  state. Which effect dominates cannot be predicted from qualitative considerations; so one has to rely on calculations for the prediction of which triplet state,  ${}^3E'$  and  ${}^3E''$ , is lower in energy.

Table 1 shows that  ${}^3E'$  and  ${}^3E''$  are, in fact, calculated to be very close in energy. Both degenerate triplet states are expected to undergo first-order Jahn–Teller distortions to  $C_{2v}$  symmetry,<sup>43</sup> and the calculated energy differences between the two triplet

states at their  $C_{2v}$  equilibrium geometries range between 1 and 3 kcal mol<sup>-1</sup>.

Interestingly, the results, tabulated in Table 1, reveal that the CCSD(T) and CASPT2 calculations differ as to which triplet state is predicted to be lower in energy. The CCSD(T) calculations predict that the  $C_{2v}$  triplet, formed by exciting an electron from the pair of  $e'$   $\sigma$  MOs into the  $a'_2$   $\sigma$  MO, is lower in energy than the triplet that is formed by exciting an electron from the pair of  $e''$   $\pi$  MOs into the  $a'_2$  MO. B3LYP makes the same prediction as CCSD(T). However, it should be noted that B3LYP erroneously predicts that both triplet states are lower in energy than the  $D_{3h}$   ${}^1A'_1$  state (Table 1).

CCSD(T) and B3LYP both predict that the  ${}^3E'$  and  ${}^3E''$  states have very similar energies at their respective  $D_{3h}$  geometries. However, as would be expected, removing an electron from one of the  $e'$   $\sigma$  MOs results in a larger Jahn–Teller distortion than removing an electron from one of the  $e''$   $\pi$  MOs. B3LYP, CCSD(T), and CASPT2 calculations all find that this is, in fact, the case. The larger energy lowering of the  ${}^3E'$  state by a first-order Jahn–Teller distortion leads to the prediction by both CCSD(T) and B3LYP that the  $C_{2v}$  distorted  ${}^3E'$  state is the lowest energy triplet state of  $CO_3$  by 2–3 kcal mol<sup>-1</sup>.

In contrast to CCSD(T), CASPT2 places  ${}^3E''$  well below  ${}^3E'$  at their respective  $D_{3h}$  geometries. Even though the first-order Jahn–Teller distortion to  $C_{2v}$  symmetry stabilizes  ${}^3E'$  more than  ${}^3E''$ , the energetic advantage of  ${}^3E''$  over  ${}^3E'$  at their respective  $D_{3h}$  geometries prevails; and the  $C_{2v}$  distorted  ${}^3E''$  ( ${}^3A_2$ ) state is calculated to be lower in energy than the  $C_{2v}$  distorted  ${}^3E'$  ( ${}^3A_1$ ) state by 1–2 kcal mol<sup>-1</sup>.

### Which triplet state is lower in energy, ${}^3E'$ ( ${}^3A_1$ ) or ${}^3E''$ ( ${}^3A_2$ )?

Which method, CCSD(T) or CASPT2, gives the correct answer to the question of what is the lowest triplet state of  $CO_3$ ,  ${}^3E' \rightarrow {}^3A_1$  or  ${}^3E'' \rightarrow {}^3A_2$ ? As described in the following paragraphs, the NIPE spectrum in Fig. 1 indicates that the CCSD(T) prediction is correct; and, although  ${}^3A_1$  and  ${}^3A_2$  are very close in energy,  ${}^3A_1$  is the lower energy of these two triplet states.

This conclusion follows from the vibrational progression seen in the low energy portion of the triplet peak. As already noted, this region of the NIPE spectrum shows a progression of  $560\text{ cm}^{-1}$ . This vibrational frequency is too low to be associated with C–O stretching, but is the right size to be due to O–C–O bending. Our calculations indicate that only  ${}^3A_1$  should show an O–C–O bending progression, so it must be the lower energy of the two closely-spaced triplet states.

The conclusion that only  ${}^3A_1$  should show an O–C–O bending progression follows from the calculated geometries of  ${}^3A_1$  and  ${}^3A_2$  and is supported by our simulations of the vibrations in the peaks due to  ${}^3A_1$  and  ${}^3A_2$  in the NIPE spectra of  $CO_3^{\cdot-}$ . Table 2 gives the bond lengths and the unique bond angle of the  $C_{2v}$  minima to which CCSD(T) and CASPT2 both predict that  ${}^3E'$  and  ${}^3E''$  distort. It is clear that both the bond lengths and the bond angles of the  ${}^3A_1$  minima of the distorted  ${}^3E'$  state deviate significantly from the equality they have at  $D_{3h}$  geometries. However, the bond angles of the  ${}^3A_2$  minima of the distorted  ${}^3E''$



**Table 2** Optimized bond lengths (Å) and bond angles (degs) at the  $C_{2v}$  geometries of the  $^3A_1$  and  $^3A_2$  states of  $CO_3$ , calculated with B3LYP, CCSD(T), and CASPT2, using the aug-cc-pVTZ basis set.  $O_1$  is the unique oxygen, and  $O_2$  and  $O_3$  are the two equivalent oxygens at  $C_{2v}$  geometries

Bond length, or bond angle	B3LYP		CCSD(T)		CASPT2	
	$^3A_1$	$^3A_2$	$^3A_1$	$^3A_2$	$^3A_1$	$^3A_2$
R(C- $O_1$ )	1.311	1.338	1.321	1.334	1.325	1.315
R(C- $O_2$ ) = R(C- $O_3$ )	1.257	1.245	1.259	1.254	1.259	1.267
$O_2$ -C- $O_3$	113.6°	122.0°	113.8°	119.2°	114.2°	119.7°
$O_1$ -C- $O_2$ = $O_1$ -C- $O_3$	123.2°	119.0°	123.1°	120.4°	122.9°	120.1°

state are calculated to remain much more nearly equal after Jahn–Teller distortions.

The difference between the geometries of the  $C_{2v}$  minima for the two triplet states is a consequence of the difference between the MOs that are occupied in these two states. In the  $^3A_1$  state an electron, which occupies the  $1b_2$   $\sigma$  MO in the  $D_{3h}$   $^1A_1'$  ground state, is removed and placed in the  $2b_2$   $\sigma$  MO. As shown in Fig. 2, this electronic excitation results in the  $O_1$ - $O_2$  and  $O_1$ - $O_3$   $\sigma$  bonding interactions in the  $1b_2$  MO being replaced by  $\sigma$  antibonding interactions between all of the oxygens in the  $2b_2$  MO. Consequently, the  $O_1$ -C- $O_2$  and  $O_1$ -C- $O_3$  bond angles in  $^3A_1$  are calculated to be larger than 120°; so the  $O_2$ -C- $O_3$  bond angle is predicted to be much less than 120° in this state.

In the  $^3A_2$  state an electron, which occupies the  $b_1$   $\pi$  MO in the  $D_{3h}$   $^1A_1'$  ground state, is removed and placed in the  $2b_2$   $\sigma$  MO. The antibonding  $O_1$ - $O_2$  and  $O_1$ - $O_3$   $\pi$  interactions in  $b_1$  are lost, as is the bonding  $O_2$ - $O_3$   $\pi$  interaction. Consequently, the  $O_1$ -C- $O_2$  and  $O_1$ -C- $O_3$  angles in the  $^3A_2$  state are expected to be less than 120°, and the  $O_2$ -C- $O_3$  angle is expected to be greater than 120°.

These qualitative expectations are fulfilled at the B3LYP level of theory. However, because the 1,3-interactions between the oxygens in  $^3A_2$  involve  $\pi$ , rather than  $\sigma$  AOs, the deviations of the B3LYP bond angles from 120° are about three times smaller in  $^3A_2$  than in  $^3A_1$ . In fact, the  $\pi$  interactions in  $^3A_2$  are so small that, in the optimized CCSD(T) and CASPT2 geometries, the deviations of the bond angles from 120° are not only less than 1° but they actually deviate from 120° in the opposite direction from the B3LYP bond angles.

In NIPE spectra progressions are only seen in vibrational modes that affect the geometrical parameters by which an electronic state differs from the radical anion from which the electronic state is formed.<sup>34</sup> The calculated O–C–O bond angles in the  $^3A_1$  state of  $CO_3$  differ significantly from those in the  $D_{3h}$  equilibrium geometry of the  $^2A_2'$  ground state of  $CO_3^{\cdot-}$ . Therefore, one would expect to see a long vibrational progression in O–C–O bending in the band for formation of the  $^3A_1$  state of  $CO_3$  in the NIPE spectrum of  $CO_3^{\cdot-}$ .

On the other hand, the calculated O–C–O bond angles in the  $^3A_2$  state of  $CO_3$  are very close to those in the  $D_{3h}$  equilibrium geometry of the  $^2A_2'$  radical anion. Therefore, one would not expect to see a long vibrational progression in O–C–O bending in the band for formation of the  $^3A_2$  state of  $CO_3$  in the NIPE spectrum of  $CO_3^{\cdot-}$ . The only long vibrational progression that

should appear in the band for formation of the  $^3A_2$  state is one in C–O bond stretch, since the C–O bond lengths in the  $C_{2v}$  equilibrium geometry of  $^3A_2$  in Table 2 differ from those in the  $D_{3h}$  equilibrium geometry of the radical anion.<sup>44</sup>

Fig. 1 shows that a vibrational progression of  $560\text{ cm}^{-1}$  in O–C–O bending is found in the band for formation of the lowest triplet state of  $CO_3$  in the NIPE spectrum of  $CO_3^{\cdot-}$ . As discussed above, such a progression is expected to be seen in the  $^3A_1$  state of  $CO_3$ , but not in the  $^3A_2$  state. Thus, it follows that the lowest triplet state of  $CO_3$  is the  $^3A_1$  state, in which one unpaired electron resides in the  $1b_2$  MO and the other resides in the  $2b_2$  MO.

This qualitative conclusion is supported by both B3LYP and CCSD(T) simulations of the triplet region of the NIPE spectrum

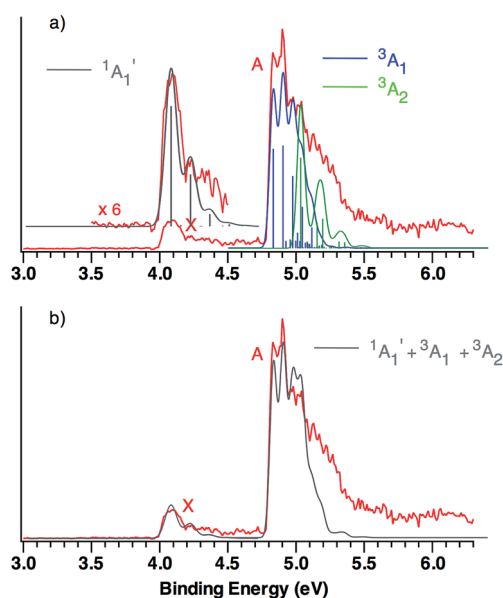


**Fig. 3** (a) B3LYP/aug-cc-pVTZ calculated vibrational structure in the NIPE spectrum of  $CO_3^{\cdot-}$ , superimposed on the experimental NIPE spectrum (red). The positions of the bands in the calculated stick spectrum for  $^1A_1'$  (grey),  $^3A_1$  (blue), and  $^3A_2$  (green) have been adjusted, in order to align the 0–0 bands in the calculated spectrum with the 0–0 bands in the observed spectrum. The calculated spectrum, using Gaussian line shapes with, respectively, 100, 60, and 60 meV full widths at half maxima for each stick in  $^1A_1'$ ,  $^3A_1$ , and  $^3A_2$ , is also shown. (b) The computed NIPE spectrum (grey), calculated from the sum of the convoluted contributions of the singlet and two triplets in Fig. 3a, superimposed on the experimental 193 nm spectrum (red).



of  $\text{CO}_3^{\cdot-}$ . Using the Franck–Condon factors (FCFs) calculated with ezSpectrum,<sup>32</sup> Fig. 3 shows how the NIPE spectrum of  $\text{CO}_3^{\cdot-}$  is predicted to appear, based on the results obtained with B3LYP calculations.

The predicted vibrational structure for the triplet region of the NIPE spectrum, based on the results of CCSD(T) calculations, has a very similar appearance to the B3LYP-based simulation in Fig. 3. The CCSD(T) simulations are provided in Fig. S1 and S2 of the ESI† of this manuscript, and the vibrational mode assignments are given in Fig. S1.† Both the B3LYP and CCSD(T) simulations confirm that the vibrational progressions in the triplet region of the experimental NIPE spectrum are dominated by the O–C–O bending mode in  $^3\text{A}_1$  and by C–O bond stretch in  $^3\text{A}_2$ .

Comparison of the simulated spectra for both triplet states with the actual NIPE spectrum suggests aligning the 0–0 band of  $^3\text{A}_2$  with the fourth resolved peak (EBE = 5.03 eV) in band A, which leads to the conclusion that the  $^3\text{A}_2$  state is 0.20 eV (4.6 kcal mol<sup>-1</sup>) higher in energy than  $^3\text{A}_1$ . This ordering of the two triplet states is in accordance with the results of both the B3LYP and CCSD(T) calculations (Table 1). However, an energy difference of 4.6 kcal mol<sup>-1</sup> would be about twice the size of the energy differences of, respectively, 2.6 and 2.3 kcal mol<sup>-1</sup> that are predicted by these two types of calculations.

An alternative alignment of the 0–0 band of  $^3\text{A}_2$  with the third resolved peak (EBE = 4.97 eV) in band A is shown in Fig. S3 of the ESI.† This alignment makes the  $^3\text{A}_2$  state only 0.14 eV (3.2 kcal mol<sup>-1</sup>) higher in energy than  $^3\text{A}_1$ , which is in better agreement with the energy differences between these two states, computed by both B3LYP and CCSD(T). However, comparison of Fig. S3† with Fig. 3, shows that the alignment in Fig. S3† fits the observed intensities of the peaks in the experimental NIPE spectrum less well than the alignment in Fig. 3.

The simulated vibrational structure for formation of the singlet ground state of  $\text{CO}_3$  is also shown in Fig. 3. The simulation reproduces well the observed vibrational progression in the singlet ground state and confirms the conclusion that this progression is due to the symmetric C–O stretching.

The simulations, based on the calculated FCFs, for formation of the singlet and two triplet states of  $\text{CO}_3$  from the  $^2\text{A}'_2$  state of  $\text{CO}_3^{\cdot-}$ , provide a good fit to the experimental NIPE spectrum of  $\text{CO}_3^{\cdot-}$  up to 5.1 eV. There appears to be a shoulder at EBE ~ 5.3 eV in the experimental spectrum, which might be due to formation of the third, low-lying triplet state,  $^3\text{A}'_2$ , which is predicted by the CCSD(T) calculations to have EA = 5.37 eV.

The similarity between the calculated and experimental NIPE spectra of  $\text{CO}_3^{\cdot-}$  in Fig. 3 provides evidence that our assignments of the peaks in the experimental NIPE spectra are correct and that, as predicted by both B3LYP and CCSD(T), the  $^3\text{A}_1$  state of  $\text{CO}_3$  is lower in energy than the  $^3\text{A}_2$  state.

## Conclusions

We report the first NIPE spectrum of  $\text{CO}_3^{\cdot-}$ . The spectrum shows that, substitution of the three oxygens in  $\text{CO}_3$  for the three  $\text{CH}_2$  groups in **TMM** results in a change in the ground state, going from  $^3\text{A}'_2$  and  $\Delta E_{\text{ST}} = 16.2$  kcal mol<sup>-1</sup> in **TMM**<sup>15</sup> to

$^1\text{A}'_1$  and  $\Delta E_{\text{ST}} = -17.8 \pm 0.9$  kcal mol<sup>-1</sup> in  $\text{CO}_3$ . The NIPE spectrum also provides the first measurement of EA = 4.06 ± 0.03 eV in  $D_{3h}$   $\text{CO}_3$ . Qualitative MO analysis and quantitative electronic structure calculations confirm that the ground state of  $\text{CO}_3$  is a singlet and reveal which of the two closely-spaced triplet excited states is lower in energy. The CCSD(T) and CASPT2 calculations reproduce the experimental EA and  $\Delta E_{\text{ST}}$  values of  $\text{CO}_3$  rather well.

The combined results of our experiments and calculations contribute fundamental information about the electronic structure of  $\text{CO}_3$ , a molecule that is not only of interest because it is isoelectronic with both **TMM** and **OXA**, but that is also important in both atmospheric chemistry and astrochemistry.<sup>12–14,45</sup>

## Conflict of interest

The authors declare no competing financial interest.

## Acknowledgements

The calculations at UNT were supported by Grant B0027 from the Robert A. Welch Foundation. The NIPES research at PNNL was supported by the U.S. Department of Energy (DOE), Office of Science, Office of Basic Energy Sciences, Division of Chemical Sciences, Geosciences and Biosciences and was performed at the EMSL, a national scientific user facility sponsored by DOE's Office of Biological and Environmental Research and located at Pacific Northwest National Laboratory, which is a multiprogram national laboratory operated for DOE by Battelle.

## Notes and references

- 1 D. Katakis and H. Taube, *J. Chem. Phys.*, 1962, **36**, 416.
- 2 A.-Y. Ung and H. I. Schiff, *Can. J. Chem.*, 1966, **44**, 1981.
- 3 N. G. Moll, D. R. Clutter and W. E. Thompson, *J. Chem. Phys.*, 1966, **45**, 4469.
- 4 E. Weissberger, W. H. Breckenridge and H. Taube, *J. Chem. Phys.*, 1967, **47**, 1764.
- 5 M. E. Jacox and D. E. Milligan, *J. Chem. Phys.*, 1971, **54**, 919.
- 6 C. S. Jamieson, A. M. Mebel and R. I. Kaiser, *ChemPhysChem*, 2006, **7**, 2508.
- 7 B. Sivaraman, B. N. R. Sekhar, D. Fulvio, A. Hunniford, B. McCullough, M. E. Palumbo and N. Mason, *J. Chem. Phys.*, 2013, **139**, 074706.
- 8 (a) B. M. Gimarc and T. S. Chou, *J. Chem. Phys.*, 1968, **49**, 4043; (b) J. F. Olsen and L. Burnelle, *J. Am. Chem. Soc.*, 1969, **91**, 7286; (c) M. Cornille and J. Horsley, *Chem. Phys. Lett.*, 1970, **6**, 373; (d) J. R. Sabin and H. Kim, *Chem. Phys. Lett.*, 1971, **11**, 593; (e) J. A. Pople, U. Seeger, R. Seeger and P. v. R. Schleyer, *J. Comput. Chem.*, 1980, **1**, 199; (f) J. S. Francisco and I. H. Williams, *Chem. Phys.*, 1985, **95**, 373.
- 9 P. LaBonville, R. Kugel and J. R. Ferraro, *J. Chem. Phys.*, 1977, **67**, 1477.
- 10 W. J. van de Guchte, J. P. Zwart and J. J. C. Mulder, *J. Mol. Struct.: THEOCHEM*, 1987, **152**, 213.



- 11 (a) M. A. Castro, S. Canuto and A. M. Simas, *Chem. Phys. Lett.*, 1991, **177**, 98; (b) R. D. J. Froese and J. D. Goddard, *J. Phys. Chem.*, 1993, **97**, 7484; (c) T. Kowalczyk and A. I. Krylov, *J. Phys. Chem. A*, 2007, **111**, 8271; (d) Y. Liu, I. B. Bersuker, W. Zou and J. E. Boggs, *J. Chem. Theory Comput.*, 2009, **5**, 2679; (e) C. Qin and T.-Y. Soo, *J. Mol. Struct.: THEOCHEM*, 2009, **897**, 32; (f) F. Grein, *J. Chem. Phys.*, 2013, **138**, 204305; (g) A. S. Averyanov, Y. G. Khait and Y. V. Puzanov, *J. Mol. Struct.: THEOCHEM*, 1999, **459**, 95.
- 12 A. M. Mebel, M. Hayashi, V. V. Kislov and S. H. Lin, *J. Phys. Chem. A*, 2004, **108**, 7983.
- 13 Review: R. I. Kaiser and A. M. Mebel, *Chem. Phys. Lett.*, 2008, **465**, 1.
- 14 C. J. Bennett, C. Jamieson, A. M. Mebel and R. I. Kaiser, *Phys. Chem. Chem. Phys.*, 2004, **6**, 735.
- 15 (a) P. G. Wenthold, J. Hu, R. R. Squires and W. C. Lineberger, *J. Am. Chem. Soc.*, 1996, **118**, 475; (b) P. G. Wenthold, J. Hu, R. R. Squires and W. C. Lineberger, *J. Am. Soc. Mass Spectrom.*, 1999, **10**, 800.
- 16 (a) T. Ichino, S. M. Villano, A. J. Gianola, D. J. Goebbert, L. Velarde, A. Sanov, S. J. Blanksby, X. Zhou, D. A. Hrovat, W. T. Borden and W. C. Lineberger, *Angew. Chem., Int. Ed.*, 2009, **48**, 8509; (b) T. Ichino, S. M. Villano, A. J. Gianola, D. J. Goebbert, L. Velarde, A. Sanov, S. J. Blanksby, X. Zhou, D. A. Hrovat, W. T. Borden and W. C. Lineberger, *J. Phys. Chem. A*, 2011, **115**, 1634.
- 17 P. G. Wenthold, J. B. Kim and W. C. Lineberger, *J. Am. Chem. Soc.*, 1997, **119**, 1354.
- 18 (a) Q. Fu, J. Yang and X.-B. Wang, *J. Phys. Chem. A*, 2011, **115**, 3201; (b) B. Chen, D. A. Hrovat, S. H. M. Deng, J. Zhang, X.-B. Wang and W. T. Borden, *J. Am. Chem. Soc.*, 2014, **136**, 3589; (c) R. C. Fort Jr, S. J. Getty, D. A. Hrovat, P. M. Lahti and W. T. Borden, *J. Am. Chem. Soc.*, 1992, **114**, 7549.
- 19 D. A. Hrovat, G.-L. Hou, X.-B. Wang and W. T. Borden, *J. Am. Chem. Soc.*, 2015, **137**, 9094.
- 20 C. D. Cappa and M. J. Elrod, *Phys. Chem. Chem. Phys.*, 2001, **3**, 2986.
- 21 R. G. Ewing and M. Waltman, *Int. J. Mass Spectrom.*, 2010, **296**, 53.
- 22 (a) D. E. Hunton, M. Hofmann, T. G. Lindeman and A. W. Castleman Jr, *J. Chem. Phys.*, 1985, **82**, 134; (b) J. T. Snodgrass, C. M. Roehl, A. M. van Koppen, W. E. Palke and M. T. Bowers, *J. Chem. Phys.*, 1990, **92**, 5935; (c) J. F. Hiller and M. L. Vestal, *J. Chem. Phys.*, 1980, **72**, 4713; (d) S. E. Novich, P. Engelking, P. L. Jones, J. H. Futrell and W. C. Lineberger, *J. Chem. Phys.*, 1979, **70**, 2652; (e) I. Dotan, J. A. Davidson, G. E. Streit, D. L. Albritton and F. C. Fehsenfeld, *J. Chem. Phys.*, 1977, **67**, 2874; (f) S. P. Hong, S. B. Woo and E. M. Helmy, *Phys. Rev. A*, 1977, **15**, 1563; (g) M. L. Vestal and G. H. Mauclaire, *J. Chem. Phys.*, 1977, **67**, 3758; (h) T. O. Tiernan and R. L. C. Wu, *Adv. Mass Spectrom.*, 1978, **7**, 136.
- 23 X.-B. Wang and L.-S. Wang, *Rev. Sci. Instrum.*, 2008, **79**, 073108.
- 24 Assuming the last phase to generate  $\text{CO}_3^{\cdot-}$  from the  $\text{Na}_2\text{CO}_3$  aqueous solutions in the electrospray ionization process is nanodroplets of waters containing one  $\text{CO}_3^{2-}$  solute, then we can estimate the ratio of  $\text{CO}_3^{2-}$  over  $\text{HCO}_3^-$  is about 0.1% from the known carbonic acid dissociation constants. Because  $\text{CO}_3^{\cdot-}$  is derived from autodetachment of  $\text{CO}_3^{2-}$ , a weak intensity of  $\text{CO}_3^{\cdot-}$  ion beam is expected.
- 25 B3LYP is a combination of Becke's 3-parameter hybrid exchange functional (A. D. Becke, *J. Chem. Phys.*, 1993, **98**, 5648) with the electron correlation functional of Lee, Yang, and Parr (C. Lee, W. Yang and R. G. Parr, *Phys. Rev. B*, 1988, **37**, 785).
- 26 (a) G. D. Purvis and R. J. Bartlett, *J. Chem. Phys.*, 1982, **76**, 1910; (b) K. Raghavachari, G. W. Trucks, J. A. Pople and M. H. Head-Gordon, *Chem. Phys. Lett.*, 1989, **157**, 479.
- 27 K. Andersson, P.-Å. Malmqvist and B. O. Roos, *J. Chem. Phys.*, 1992, **96**, 1218.
- 28 W. T. Borden and E. R. Davidson, *Acc. Chem. Res.*, 1996, **29**, 87.
- 29 (a) T. H. Dunning Jr, *J. Chem. Phys.*, 1989, **90**, 1007; (b) R. A. Kendall, T. H. Dunning Jr and R. J. Harrison, *J. Chem. Phys.*, 1992, **96**, 6769.
- 30 M. J. Frisch, G. W. Trucks, H. B. Schlegel, G. E. Scuseria, M. A. Robb, J. R. Cheeseman, G. Scalmani, V. Barone, B. Mennucci, G. A. Petersson, H. Nakatsuji, M. Caricato, X. Li, H. P. Hratchian, A. F. Izmaylov, J. Bloino, G. Zheng, J. L. Sonnenberg, M. Hada, M. Ehara, K. Toyota, R. Fukuda, J. Hasegawa, M. Ishida, T. Nakajima, Y. Honda, O. Kitao, H. Nakai, T. Vreven, J. A. Montgomery Jr, J. E. Peralta, F. Ogliaro, M. Bearpark, J. J. Heyd, E. Brothers, K. N. Kudin, V. N. Staroverov, T. Keith, R. Kobayashi, J. Normand, K. Raghavachari, A. Rendell, J. C. Burant, S. S. Iyengar, J. Tomasi, M. Cossi, N. Rega, N. J. Millam, M. Klene, J. E. Knox, J. B. Cross, V. Bakken, C. Adamo, J. Jaramillo, R. Gomperts, R. E. Stratmann, O. Yazyev, A. J. Austin, R. Cammi, C. Pomelli, J. W. Ochterski, R. L. Martin, K. Morokuma, V. G. Zakrzewski, G. A. Voth, P. Salvador, J. J. Dannenberg, S. Dapprich, A. D. Daniels, O. Farkas, J. B. Foresman, J. V. Ortiz, J. Cioslowski and D. J. Fox, *Gaussian 09, Revision D.01*, Gaussian, Inc., Wallingford CT, 2013.
- 31 K. Andersson, F. Aquilante, M. Barysz, A. Bernhardsson, M. R. A. Blomberg, Y. Carissan, D. L. Cooper, M. Cossi, L. DeVico, N. Ferré, M. P. Fülscher, A. Gaenko, L. Gagliardi, G. Ghigo, C. de Graaf, S. Gusarov, B. A. Hess, D. Hagberg, A. Holt, G. Karlström, R. Lindh, P.-Å. Malmqvist, T. Nakajima, P. Neogrády, J. Olsen, T. Pedersen, M. Pitonak, J. Raab, M. Reiher, B. O. Roos, U. Ryde, B. Schimmelpfennig, M. Schütz, L. Seijo, L. Serrano-Andrés, P. E. M. Siegbahn, J. Stålring, T. Thorsteinsson, V. Veryazov and P.-O. Widmark, *MOLCAS version 7*, Lund University, Sweden, 2008.
- 32 V. A. Mozhayskiy and A. I. Krylov, *ezSpectrum, version 3.0*, see <http://iopshell.usc.edu/downloads>.
- 33 (a) J. Franck, *Trans. Faraday Soc.*, 1926, **21**, 536; (b) E. Condon, *Phys. Rev.*, 1926, **28**, 1182.
- 34 Reviews: (a) L. C. Lineberger and W. T. Borden, *Phys. Chem. Chem. Phys.*, 2011, **13**, 11792; (b) W. T. Borden, in *Fifty Years of the James Flack Norris Award*, ed. E. T. Strom and V. Mainz, American Chemical Society, Washington, DC, in press.





- 35 (a) W. T. Borden and E. R. Davidson, *J. Am. Chem. Soc.*, 1977, **99**, 4587; (b) W. T. Borden, in *Diradicals*, ed. W. T. Borden, Wiley-Interscience, New York, 1982, pp. 1–72.
- 36 Review: W. Kutzelnigg, *Angew. Chem., Int. Ed. Engl.*, 1996, **35**, 573 and references therein.
- 37 Because the  $a_2''$   $\pi$  lone-pair MO contains bonding interactions between the  $2p$ - $\pi$  lone-pairs on the oxygens and the  $2p$ - $\pi$  AO on the carbon, it is considerably lower in energy than the  $\sigma$  and  $\pi$  lone-pair MOs on oxygen that are shown in Fig. 2.
- 38 As found previously,<sup>20</sup> a  $C_{2v}$  structure for  $\text{CO}_3^{3-}$  is computed to be higher in energy than the  $D_{3h}$  structure.
- 39 Review: E. R. Davidson and W. T. Borden, *J. Phys. Chem.*, 1983, **87**, 4783.
- 40 For more recent discussions of artifactual symmetry breaking in  $D_{3h}$  molecules, see (a) W. Einfeld and K. Morokuma, *J. Chem. Phys.*, 2000, **113**, 5587; (b) C. E. Miller and J. W. Francisco, *J. Phys. Chem. A*, 2001, **105**, 1662; (c) Ref. 21.
- 41 Artifactual symmetry breaking leads to another phenomenon that can be seen in the results given in Table 1 for the triplet states. At  $D_{3h}$  geometries the  $E'_x$  and  $E'_y$  components of the  ${}^3E'$  state should have identical energies, as should the  $E''_x$  and  $E''_y$  components of the  ${}^3E''$  state. The fact that the two components of each degenerate state do not have exactly the same energies in Table 1 can be viewed as a consequence of the fact that, in general, electronic structure codes impose only  $C_{2v}$  symmetry on the MOs used to construct  $D_{3h}$  wave functions. Consequently, a wave function that nominally has  $E_x$  symmetry actually contains an  $A_2$  contaminant; and a wave function that nominally has  $E_y$  symmetry actually contains an  $A_1$  contaminant. Although the  $E_x$  and  $E_y$  components of such wavefunctions do have the same energies, the  $A_2$  and  $A_1$  contaminants do not; and this leads to the energy differences at  $D_{3h}$  geometries between the “ $E_x$ ” and “ $E_y$ ” states in Table 1.<sup>39a</sup>
- 42 See, *inter alia*, (a) U. Öpik and M. H. L. Pryce, *Proc. R. Soc. London, Ser. A*, 1957, **238**, 425; (b) R. F. W. Bader, *Can. J. Chem.*, 1962, **40**, 1164; (c) R. G. Pearson, *J. Am. Chem. Soc.*, 1969, **91**, 4947; (d) R. G. Pearson, *J. Mol. Struct.*, 1983, **103**, 25. For a recent review see: (e) I. B. Bersuker, *Chem. Rev.*, 2013, **113**, 1351.
- 43 H. A. Jahn and E. Teller, *Proc. R. Soc. London, Ser. A*, 1937, **161**, 220.
- 44 A similar situation occurs in the lowest energy triplet state of  $(\text{CO})_5$ , which undergoes a first-order Jahn–Teller distortion from the  $D_{5h}$  geometry of the radical anion. The expected C–C bond stretching progression is, in fact, seen in the NIPE spectrum of  $(\text{CO})_5^{3-}$  in the band for formation of the lowest triplet state of  $(\text{CO})_5$ . X. Bao, D. A. Hrovat, W. T. Borden and X.-B. Wang, *J. Am. Chem. Soc.*, 2013, **135**, 4291.
- 45 C. J. Bennett, C. S. Jamieson and R. I. Kaiser, *Phys. Chem. Chem. Phys.*, 2010, **12**, 4032.

